10-1-1994

Nondestructive Mapping of Carrier Concentration and Dislocation Density in N(+)-Type GaAs

David C. Look
Wright State University - Main Campus, david.look@wright.edu

D. C. Walters

M. G. Mier

J. R. Sizelove

Nondestructive mapping of carrier concentration and dislocation density in n^+-type GaAs

D. C. Look and D. C. Walters
University Research Center, Wright State University, Dayton, Ohio 45435

M. G. Mier and J. R. Sizelove
Solid State Electronics Directorate, Wright Laboratory, WL/ELRA, Wright–Patterson Air Force Base, Ohio 45433

(Received 16 June 1994; accepted for publication 22 August 1994)

Transmission mappings (500 μm×500 μm resolution) at wavelengths of 0.9–1.5 μm on 3 in., n^+-GaAs wafers ($n\simeq 1-2\times10^{18}$ cm^{-3}) correlate well with carrier concentration n, measured by the Hall effect, and dislocation density, as confirmed by KOH etch-pit patterns. The absorption for $\lambda\gtrsim1.0$ μm (below band edge) varies directly with n via free-carrier interconduction-band transitions, while the absorption for $\lambda\lesssim0.95$ μm (near band edge) varies inversely with n because of band-filling effects. Both phenomena are highly useful for n^+-GaAs wafer characterization. © *1994 American Institute of Physics.*

Transmission maps have proved to be very useful in delineating variations of EL2 concentration [EL2],[1–3] dislocation density ρ_D,[4,5] and stress[6] in semi-insulating (SI) GaAs wafers. It has been possible in some cases to correlate such maps of material properties with maps of device properties from the same (or an adjacent) wafer.[1,7] While the [EL2] and stress measurements are nondestructive, the ρ_D measurements require a KOH etch to form etch pits at the surface. In contrast to the EL2 centers, which reduce the transmission by absorption, the etch pits reduce the transmission by scattering; however, both effects are easily quantifiable. A long sought goal in the semiconductor industry has been a convenient technique for nondestructive evaluation of dislocation density. However, none of the usual optical techniques have proved to be useful for this purpose so far.

For n^+-GaAs wafers, used in the fabrication of lasers, solar cells, and other devices, it seems that very little whole-wafer characterization has been carried out in the past. In n^+-GaAs, [EL2] is very small and not important, but the dislocations are even more important than in SI GaAs because they can lead to dark-line defects and other nonradiative recombination centers which are deleterious to lasers. Also of importance is n, because high n produces two desirable device properties, namely, low series resistance, and good ohmic contacts. In this letter we show that both n and ρ_D can be precisely mapped nondestructively in n^+-GaAs wafers.

The n^+ wafers analyzed in this study were grown by the vertical gradient freeze technique and doped with approximately 2×10^{18} cm^{-3} Si. They were about 635 μm thick and polished on both sides. Transmission maps at wavelengths between 0.89 and 1.5 μm, with 0.02 μm resolution, were achieved by moving the wafer in controlled steps between the exit slit of a 1/4 m Bausch and Lomb monochromator, and a cooled Ge detector. Signal to noise was enhanced by chopping the light and using phase-sensitive detection. Resolution was 500 μm×500 μm, which translates to about 16 000 points on a 3 in. wafer.

To *directly* study dislocation density, a wafer was etched in molten KOH (400 °C, 45 min), which produces a hexagonal pit at each point for which a dislocation intersects the surface. Both the unetched and etched wafers were analyzed by the following formula:[5]

$$T=\frac{(1-R)^2(1-S)^2e^{\alpha d}}{1-R^2(1-S)^2e^{-2\alpha d}}, \tag{1}$$

where T is the relative transmission, S is the scattering factor ($S\simeq0$ for an unetched wafer), α is the absorption coefficient, d is the sample thickness, and R is the reflection coefficient, given approximately by $R=(\eta-1)^2/(\eta+1)^2$ in our wavelength range. Here η, the real part of the refractive index, approximately obeys[8]

$$\eta=\left[7.10+\frac{3.78}{1-0.18(h\nu)^2}\right]^{1/2} \tag{2}$$

at 300 K, where $h\nu$ is the light energy in eV.

It is well known[9,10] that $\alpha\propto n$ in GaAs for $\lambda\geqslant1$ μm and $n\geqslant5\times10^{17}$ cm^{-3}. To check this relationship and calibrate our wafers, we cut 20 6 mm×6 mm pieces from positions along the horizontal and vertical diameters of the wafer, and determined n on each piece by Hall-effect measurements. These values of n were compared with respective average values of α(1.5 μm) calculated from Eq. (1) at the 144 positions (1/2 mm×1/2 mm resolution) comprising the space of each 6 mm×6 mm Hall piece. The map of α(1.5 μm) is shown in Fig. 1(a), and the correlation plot with n obeys

$$\alpha=0.81+4.0\times10^{-18}n, \tag{3}$$

with a correlation coefficient of 0.94. The slope, $d\alpha/dn\simeq4\times10^{-18}$ cm^2 at $\lambda=1.5$ μm, can be compared with the value $d\alpha/dn\simeq6\times10^{-18}$ cm^2 at $\lambda=2$ μm, deduced from earlier data.[8,9] These results are not inconsistent considering the different wavelengths and the errors inherent in each measurement. Note that α in Fig. 1(a) does not have either radial or fourfold symmetry as a *dominant* feature in this particular wafer. The map of α at 0.9 μm, shown in Fig. 1(b), strongly emphasizes five regions, in the center and along diagonal [100] diameters, which were nearly hidden in the

 0003-6951/94/65(17)/2188/3/$6.00

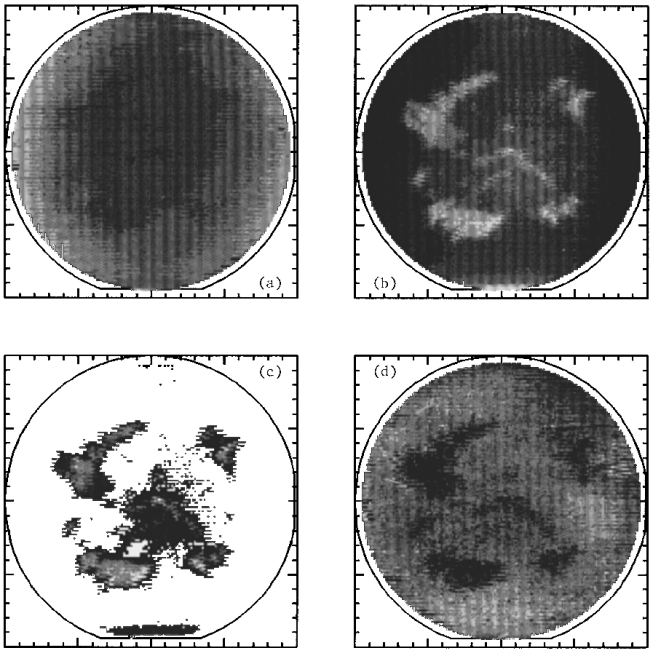

FIG. 1. (a) A map of absorption coefficient α at wavelength $\lambda=1.5$ μm; the gray scale covers $\alpha=6.6$–9.5 cm^{-1}, with black highest; (b) α at 0.9 μm, gray scale 46.3–51.3 cm^{-1}; (c) regions of α (0.9 μm) for which $\alpha\lesssim 48.3$ cm^{-1}, gray scale 46.3–48.3 cm^{-1}; (d) fractional scattering S at $\lambda=0.9$ μm, gray scale 0.19–0.33.

1.5 μm map [Fig. 1(a)]. These are regions of slightly higher n and thus slightly higher α for $\lambda=1.5$ μm. However, at 0.9 μm the contrast is reversed, i.e., the regions of higher n produce lower α. The five regions can be separated from the background by simply mapping only the lowest range of $\alpha(\alpha\simeq 46$–48 cm^{-1}), shown in Fig. 1(c). Such a separation ("filtering") is possible because of the very high contrast shown in these regions at $\lambda=0.9$ μm. A correlation plot of the full 0.9 μm map [Fig. 1(b)] with n gives

$$\alpha=61-6.5\times 10^{-18}n, \tag{4}$$

with a correlation coefficient of 0.95. Note that $d\alpha/dn$ is larger at $\lambda=0.9$ μm than at $\lambda=1.5$ μm, and this explains the better contrast in Fig. 1(b) as compared to that in Fig. 1(a).

This same wafer was etched in KOH and analyzed again at 0.9 μm. Since this procedure affects only the surface, α remains the same; however, now $S\neq 0$, because the etch pits scatter the light. Since α is the same, we were able to use Eq. (1) to calculate the scattering factor S at each point, and the map of S is shown in Fig. 1(d). Obviously, the five regions of low α in the unetched, 0.9-μm maps [Figs. 1(b) and 1(c)] correspond almost exactly with the five regions of high scattering in the etched wafer. The same type of scattering calculation was also carried out for the 1.5 μm absorption data on the etched wafer, and the $S(1.5$ μm) map (not shown) was found to be nearly identical to the $S(0.9$ μm) map. Observation under a microscope and manual EPD counting confirmed that the five regions were indeed the only regions with etch pits (maximum about 1500 cm^{-2}); in fact, most of the wafer was dislocation-free.

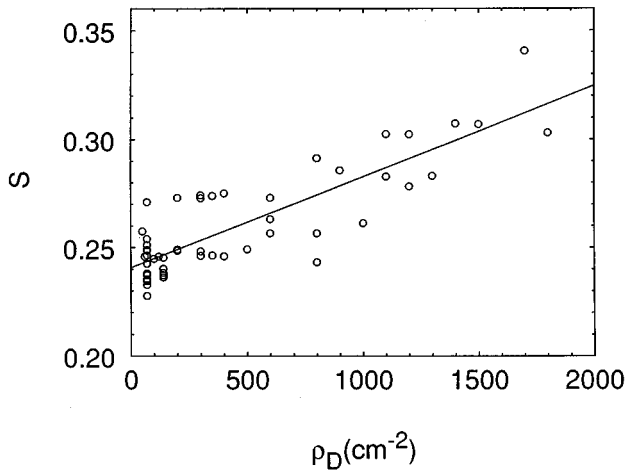

FIG. 2. Scattering factor S at 0.9 μm vs the manually counted dislocation density ρ_D.

In a previous report,[5] we showed that $S\simeq S_0+\beta(1-e^{-a\rho_D})$, where S_0 is the background scattering due to causes other than etch pits, β the fraction of light scattered out of the detector acceptance angle by an etch pit ($\beta=0$–1), and a the average area of an etch pit. In this case, $a\simeq 1.3\times 10^{-4}$ cm^2, and since the maximum ρ_D is about 10^3 cm^{-2}, $a\rho_D\ll 1$ so that $dS/d\rho_D\simeq\beta a\simeq 1.3\times 10^{-4}\beta$ cm^2. A correlation plot of $S(0.9$ μm) versus the manually counted ρ_D, shown in Fig. 2 (correlation coefficient=0.82), gives

$$S=5.6\times 10^{-5}\rho_D+0.24, \tag{5}$$

which agrees with the theoretical estimate above if $\beta\simeq 0.4$ -0.5, a reasonable range. The "excess" scattering, $S_0\simeq 0.24$, is due to the overall surface roughening by the KOH etch, even in regions where no etch pits are formed.

The possibility of determining ρ_D *nondestructively* can be demonstrated by plotting $\alpha(0.9$ μm) versus the manually counted ρ_D, shown in Fig. 3. The result is

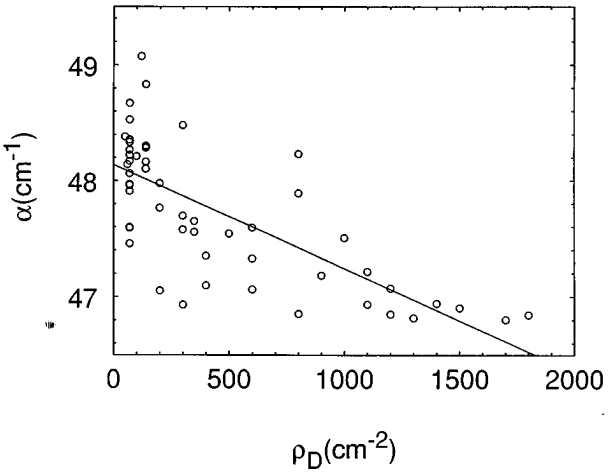

FIG. 3. Absorption α at 0.9 μm vs the manually counted dislocation density ρ_D.

$$\alpha = A - B\rho_D = 48 - 1.5\times 10^{-3}\rho_D, \quad (6)$$

with a correlation coefficient of 0.76. The scatter in the plot is relatively high because of large statistical variations in the manual etch pit counting due to the small etch-pit density. Obviously, the term A should depend upon n, and B may also. Thus studies on other wafers will need to be carried out to establish these parameters for other ranges of n. However, even without calibration, it is still very useful to be able to delineate the regions of high dislocation density, as shown in Fig. 1(b) and 1(c).

The explanation for these phenomena is as follows. In the region $\lambda = 1.0$–1.5 μm, the absorption is due to interconduction-band transitions of the free carriers,[10] i.e., transitions such as $\Gamma_1 \rightarrow \Gamma_{15} \rightarrow X_1$. The $\Gamma_{15} \rightarrow X$ transitions require phonons for momentum conservation and, indeed, 300 K is a high enough temperature to provide the phonons. The theoretical wavelength dependence is relatively weak, as confirmed in our samples, although α from this mechanism falls off rapidly above 3 μm since the light energy becomes too low to cause interband excitation. Thus $\alpha \propto n$ at $\lambda = 1.0$–1.5 μm.

As the light energy approaches the band edge [$E_g \simeq 1.424$ eV (0.870 μm) at 300 K, for small n], valence- to conduction-band transitions begin to dominate, and thus the important parameter for absorption is $E_g(\lambda,n)$. Suppose we model $\alpha = f(h\nu - E_g)$; then $d\alpha/d(h\nu) = -d\alpha/dE_g$. We can experimentally vary $h\nu$ around 0.9 μm (1.377 eV); the result, in a region away from the high dislocation regions, is $d\alpha/d(h\nu) \simeq -d\alpha/dE_g \simeq 950$ cm^{-1}/eV. We found earlier, Eq. (4), that $d\alpha/dn = -6.5\times 10^{-18}$ cm^{-1}/cm^{-3} at 0.9 μm. Thus we get $dE_g/dn \simeq 6.8\times 10^{-21}$ eV/cm^{-3}. It must be remembered that this is the *effective* E_g, i.e., E_{ge}, as measured from the valence band to the Fermi level E_F, which is well above the conduction-band edge at $n = 2\times 10^{18}$ cm^{-3}. As discussed by Bennett,[11] the effective band gap E_{ge} is reduced by the many body effects of carrier–carrier and carrier–donor interactions, and E_{ge} is increased by carrier band filling (Moss–Burstein effect[12,13]). At $n = 1.5$–2.0×10^{18} cm^{-3}, the net result of these two effects is $dE_{ge}/dn = 1.0\times 10^{-20}$ eV/cm^{-3}, as deduced from Fig. 16 of Bennett's paper. It should be mentioned that Bennett's E_{ge} is the value appropriate for calculation of the intrinsic carrier concentration, whereas our E_{ge} is that appropriate for optical transitions. Within these constraints, theory and experiment are in good agreement.

The reason that n increases in regions of high ρ_D may result from As-rich stoichiometry, as is the case with undoped, semi-insulating GaAs.[14] That is, an As-rich region will likely have an excess of Ga vacancies, which will promote Si on the Ga site (Si_{Ga}), a donor, rather than Si_{As}, an acceptor. This phenomenon is known to be operative in Si-implanted GaAs.[15] Thus n will increase and $\alpha(0.9\ \mu\text{m})$ will decrease (because of the Moss–Burstein effect)[12,13] in high-ρ_D areas of the wafer. Further experiments will have to be carried out to determine the dependence of the α-ρ_D relationship on n and other factors, but it is clear that our new technique provides an excellent nondestructive way to map ρ_D.

We wish to thank T. A. Cooper for electrical measurements, L. V. Callahan for technical assistance, and N. Blair and R. Heil for manuscript preparation. D. C. L. and D. C. W. were supported under USAF Contract No. F33615-91-C-1765 and all of the work was performed at the Solid State Electronics Directorate, Wright Laboratory.

[1] P. Dobrilla, J. S. Blakemore, A. J. McCamant, K. R. Gleason, and R. Y. Koyama, Appl. Phys. Lett. **47**, 602 (1985).
[2] F. X. Zach and A. Winnacker, Jpn. J. Appl. Phys. **28**, 957 (1989).
[3] S. K. Brierley and D. S. Lehr, Appl. Phys. Lett. **55**, 2426 (1989).
[4] P. Dobrilla and J. S. Blakemore, J. Appl. Phys. **60**, 169 (1986).
[5] D. C. Look, D. C. Walters, J. S. Sewell, S. C. Dudley, M. G. Mier, and J. R. Sizelove, J. Appl. Phys. **65**, 1375 (1989).
[6] P. Dobrilla and J. S. Blakemore, Appl. Phys. Lett. **48**, 1303 (1986).
[7] D. C. Look, D. C. Walters, R. T. Kemerley, J. M. King, M. G. Mier, J. S. Sewell, and J. R. Sizelove, J. Electron. Mater. **18**, 487 (1989).
[8] J. S. Blakemore, J. Appl. Phys. **53**, R123 (1982).
[9] W. G. Spitzer and J. M. Whelan, Phys. Rev. **114**, 59 (1959).
[10] A. S. Jordan, J. Appl. Phys. **51**, 2218 (1980).
[11] H. S. Bennett, J. Appl. Phys. **60**, 2866 (1986).
[12] T. S. Moss, Proc. Phys. Soc. London, Sect. B **67**, 775 (1954).
[13] E. Burstein, Phys. Rev. **93**, 632 (1954).
[14] K. Yamada and J. Osaka, J. Appl. Phys. **63**, 2609 (1988).
[15] F. Hyuga, K. Watanabe, J. Osaka, and K. Hoshikawa, Appl. Phys. Lett. **48**, 1742 (1986).